CONF-8404103--2

# SULFUR AND ANTIMONY SEGREGATION TO CREEP CAVITY SURFACES IN Ni AND AN FCC Fe-Ni-Cr ALLOY

CONF-8404103--2

DE84 011458

C. L. White, J. H. Schneibel, and M. H. Yoo

Metals and Ceramics Division, Oak Ridge National Laboratory
Oak Ridge, Tennessee 37831, U.S.A.

## 1. SUMMARY

Segregation of S and Sb to the internal free surfaces of creep induced cavities and microcracks in Ni and an Fe + 15% Ni + 15% Cr alloy* have been studied using scanning Auger electron spectroscopy (AES). Residual S is found to segregate strongly in the undoped Fe + 15% Ni + 15% Cr while Fe + 15% Ni + 15% Cr + 1% Sb exhibited only Sb segregation. Both S and Sb segregated in Ni + 0.15% Sb.

## 2. INTRODUCTION

Small concentrations of low melting point metalloid impurities, such as S, Sb, Sn, and As, are often observed to reduce the creep ductility of otherwise ductile alloys at temperatures between 0.4 and 0.7 $T_m$. The failure mode associated with this impurity effect usually involves formation, growth and interlinkage of cavities and microcracks on grain boundaries. Because the metalloid elements that cause this ductility loss are known to segregate to free surfaces and grain boundaries in a variety of alloy systems, it is generally accepted that the mechanism for enhanced cracking and cavitation at grain boundaries involves such segregation [1–6]. The details of this mechanism are far from clear, however. Some of the interfacial properties that will be influenced by metalloid segregation are: (a) grain boundary and surface energies; (b) grain boundary and surface diffusivities; (c) grain boundary sliding; and (d) grain boundary migration.

These properties interact in a complex fashion to influence the nucleation, growth, and interlinkage of the

*Unless otherwise specified, all percentages will be "by mass."

cavities and microcracks that lead to low ductility failure. The purpose of this paper is to present experimental observations of metalloid segregation to surfaces of creep-induced grain boundary cavities and microcracks in Ni and an Fe + 15% Ni + 15% Cr alloy. Interested readers are referred to a recent review of segregation effects on creep cavitation for mechanistic interpretation of such results [3].

## 3. EXPERIMENTAL

### 3.1 Alloys

Fe + 15% Ni + 15% Cr alloys with and without 1% Sb, and one Ni + 0.15% Sb alloy, were prepared from high purity melt stock by arc melting and drop casting (AMDC) under argon. A second Ni + 0.15% Sb alloy was prepared from commercial Ni-201 that was levitation-floating-zone refined (LFZR), then doped with a Ni-Sb master alloy and zone-leveled. All alloys were cold swaged to 9.5 mm or 6.4 mm diam and machined into tensile specimens.

Chemical analyses for S and Sb are summarized for each alloy in Table 1. Analysis for Ni, Cr, and C in the Fe + 15% Ni + 15% Cr alloys indicated 14.4, 15.4, and 0.025% respectively. Transmission electron microscopy indicated that essentially all of the C was in solution at the 827°C creep test temperature. The LFZR-Ni + 0.15% Sb alloy was found to contain 0.1% each of Mo, Mn, and Fe, which were below 10 wt ppm in the AMDC-Ni + 0.15% Sb.

### 3.2 Creep Tests

Prior to creep testing in vacuum, the Ni + 0.15% Sb was vacuum annealed 1 h at 1000°C, and Fe + 15% Ni + 15% Cr alloys were annealed 2 h at 1050° C. Fe + 15% Ni + 15% Cr alloys were tested at 827°C and 30 MPa. Ni + 0.15% Sb alloys were tested at 595°C and 100 MPa to permit comparison with previous results on a Ni + 1% Sb alloy [4,5,6].

### 3.3 Segregation Measurements

Segregation was measured using a scanning Auger electron spectroscopy (AES) system with a spatial resolution of about 200 nm. This technique is useful for analyses of segregation to free surfaces (and internal interfaces that can be exposed as free surfaces) because its sampling depth (~1 nm) is approximately equal to the thickness of a solute-enriched region at a segregated interface. Applications of AES to segregation studies are described elsewhere [5,6,7].

All of the creep failures in this study occurred primarily by formation of grain boundary cracks and cavities

in the manner described in Sect. 2. The cavitated gage sections of failed creep specimens were then notched 3 to 4 mm from the creep fracture surface and re-fractured inside the AES analysis chamber at a pressure of approximately $10^{-8}$ Pa. The fracture device was cooled with flowing liquid nitrogen, but no attempt was made to monitor the specimen temperature during fracture.

The AES fractures were not intergranular but involved transgranular rupture of the intercavity ligaments in a manner similar to that depicted schematically in Fig. 1 [the "whiskers" in this schematic simply serve to label those portions of the AES fracture surface (f), which started out as creep-cavity surfaces (a)]. The resulting AES spectra, therefore, give information concerning the surface composition of cavities and intercavity ligaments, the latter of which should be representative of the bulk alloy. In general, information regarding segregation to grain boundaries could not be obtained from these analyses. Auger spectra were analyzed by measuring peak-to-peak intensities of the principal peak for each element detected, then correcting this intensity for differences in elemental sensitivity, and normalizing the analysis to 100 at. % [6,8].

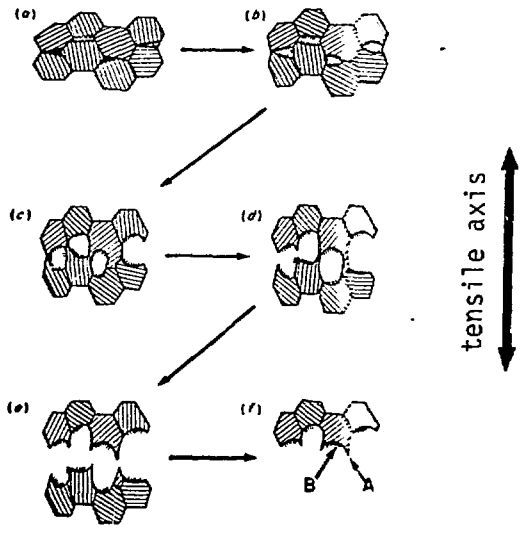


FIG. 1. Schematic representation showing rupture of intercavity ligaments during AES fracture of a creep cavitated gage section.

Following analysis of the as-fractured surface, each specimen was sputter etched using 5 keV $Ar^+$ ions to remove the top few (<10) atom layers from the surface. The underlying material was then analyzed to gain information concerning the depth of any solute-enriched regions on the AES fracture surface. Upon removal from the AES analysis chamber, the specimens were examined in a scanning electron microscope (SEM) to observe in more detail the areas previously analyzed using AES.

## 4. RESULTS

### 4.1 Fe + 15% Ni + 15% Cr

In spite of its large elongation to failure ($\varepsilon_f$ = 52% in creep at 827°C, 30 MPa), the undoped alloy failed primarily as a result of grain boundary cracking and cavitation as shown in Fig. 2. The AES fracture surface from the internally cracked gage section consisted of rounded depressions surrounded by ridges such as those identified at points B and A, respectively, in Fig. 3(a). In general, we interpret these rounded depressions as containing the cavity or crack surfaces formed during creep, while ridges are taken to represent the failed intercavity ligaments (compare to points B and A respectively in Fig. 1(f).

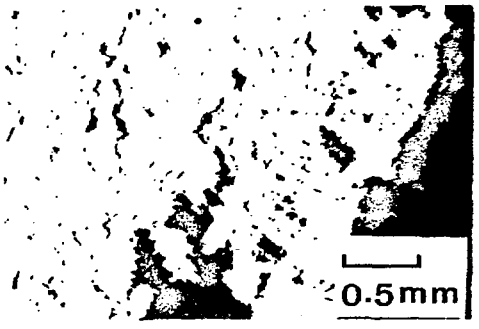


FIG. 2. Optical micrograph of Fe + 15% Cr crept to failure at 827°C, 30 MPa.

Auger spectra obtained from points A and B of Fig. 3(b) are shown in Fig. 4. AES analysis on the cavity surface showed a large peak due to S, in addition to the Fe, Ni, and Cr in the alloy. Semiquantitative analysis of this spectrum yields a S concentration of approximately 23 at. % in the top few atom layers of the cavity surface. The cavity surfaces also were slightly enriched with Cr and depleted in Ni compared to the ligaments, which are taken to be representative of the bulk.

Auger spectra of the ruptured intercavity ligaments (e.g. top spectrum in Fig. 4) showed only peaks arising from Fe, Ni, and Cr. Semiquantitative analysis of these spectra yielded average Ni and Cr concentrations of 14.7 and 16.7 at. % respectively. These values are within 8 and 2%, respectively, of the wet chemistry values for Ni and Cr in this alloy.

Figure 3(b) shows a secondary electron detector (SED) image from the fracture surface obtained during AES analysis. Figure 3(c) shows a S-Auger map over the same area, obtained by using the intensity of the 150 eV S Auger peak to modulate the brightness of the map. The map shows that the S-enriched areas on the surface are generally located within the rounded depressions that we have identified as containing the creep-induced grain boundary cracks and cavities.

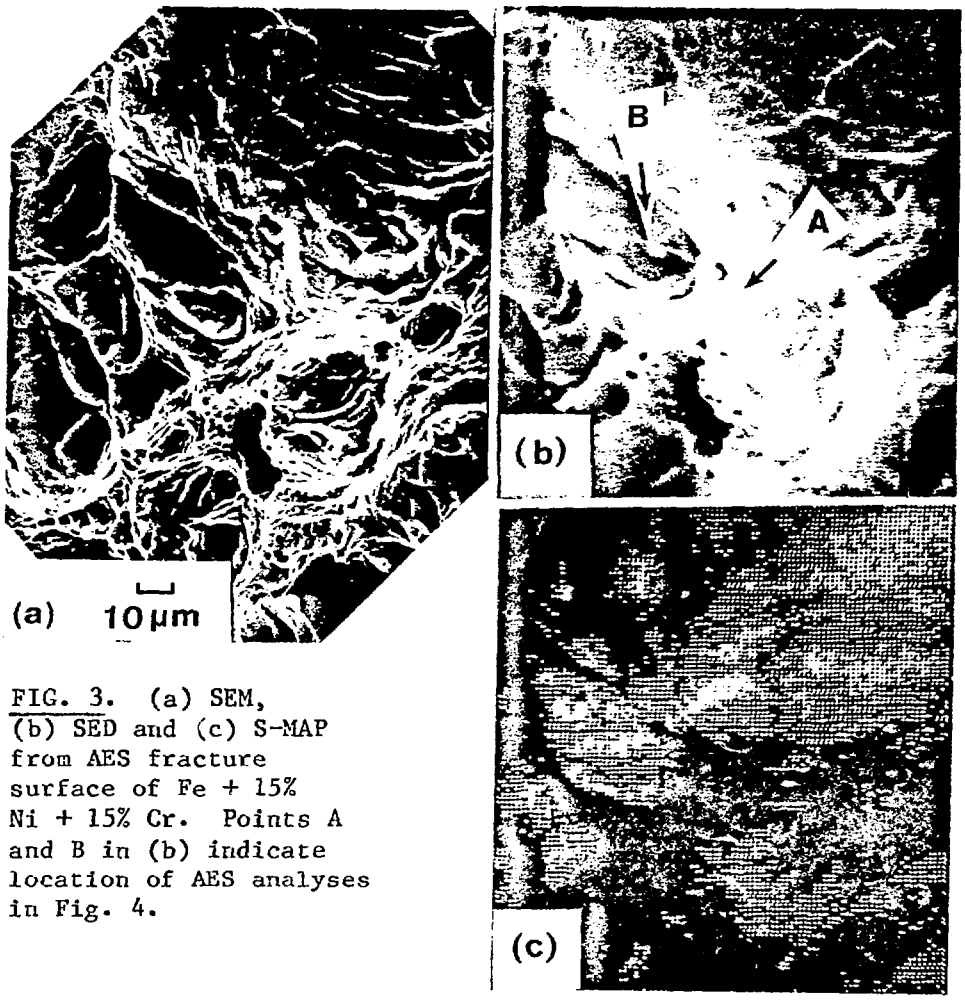


FIG. 3. (a) SEM, (b) SED and (c) S-MAP from AES fracture surface of Fe + 15% Ni + 15% Cr. Points A and B in (b) indicate location of AES analyses in Fig. 4.

The bottom spectrum in Fig. 4 was taken from the same point on the cavity surface as the center spectrum, after the fracture surface had been sputter etched to remove less than ten atom layers. Comparison of these two spectra indicates that virtually all of the S on the cavity surface is concentrated within the top few atom layers.

4.2 Fe + 15% Ni + 15% Cr + 1% Sb

The Sb doped alloy exhibited much lower $\epsilon_f$ (=18%) and more extensive grain boundary cavitation than did the undoped Fe + 15% Ni + 15% Cr alloy. The AES fracture surface of this specimen was similar in appearance to the one for the undoped alloy. The SEM image in Fig. 5 shows one of the cavity surfaces (point B) and ruptured ligaments (point A) where the Auger spectra of Fig. 6 were obtained. The spectrum from the ruptured ligament contained peaks due to Fe, Ni, and Cr only. Analysis of the spectrum yields values

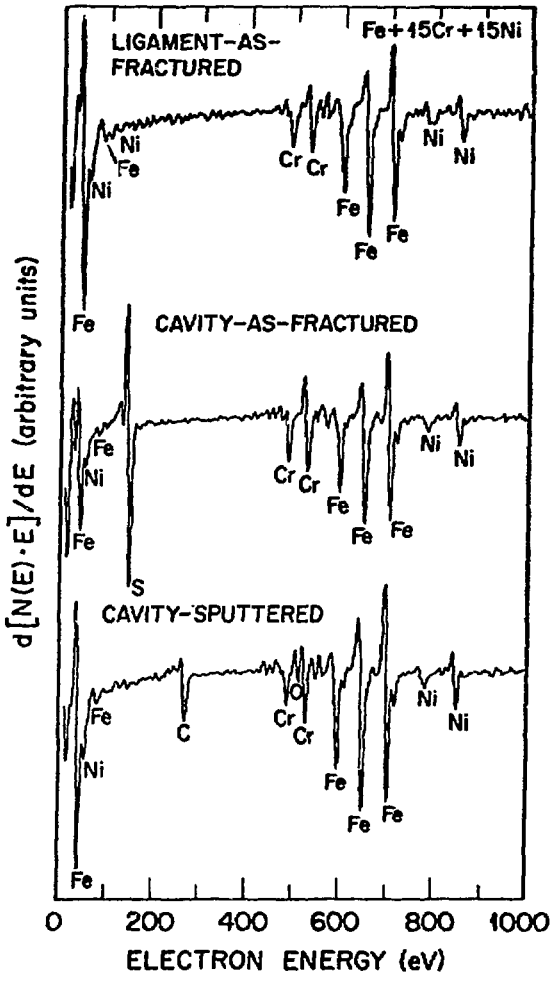


FIG. 4. Auger spectra from points A (ligament) and B (cavity) of Fig. 3.

of Ni and Cr within 4% of the values from wet chemistry. The center spectrum in Fig. 6 is from the as fractured cavity surface, and contains a large peak due to Sb at about 460 eV. Analysis of this spectrum indicates approximately 10 at. % Sb in the top few atom layers of the cavity surface. Comparison of Ni and Cr values on cavities and ligaments indicated that, in contrast to the undoped alloy, the cavity surfaces in the Sb doped alloy were slightly enriched in Ni and depleted in Cr relative to the bulk. Sputter etching and reanalysis of the cavity surfaces again indicated that the solute-enriched region was only a few atom layers thick.

FIG. 5. SEM showing AES fracture of Fe + 15% Ni + 15% Cr + 1% Sb. Points A (ligament) and B (cavity) indicates location of AES analyses in Fig. 6.

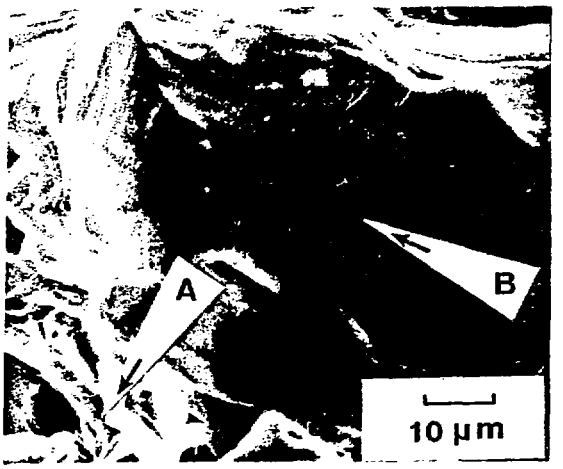


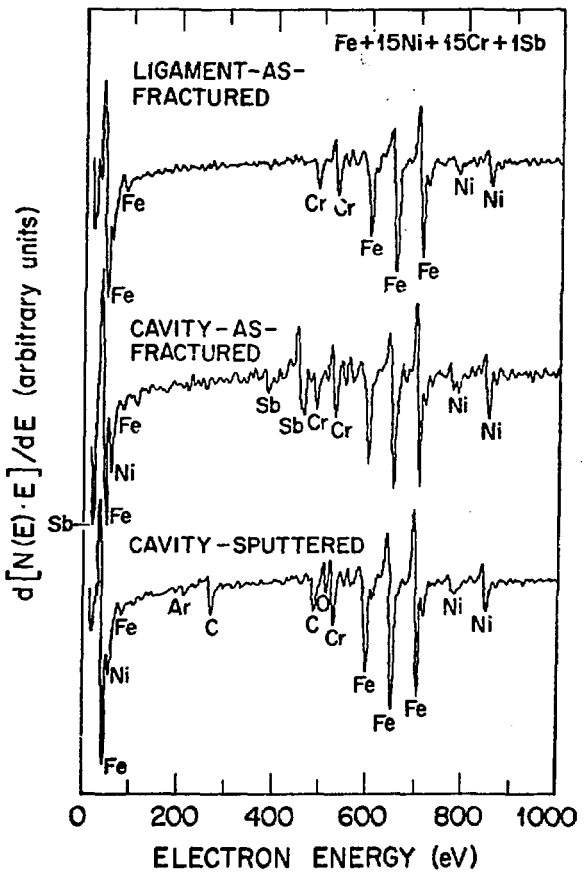


FIG. 6. Auger spectra from points A (ligament) and B (cavity) of Fig. 5.

4.3 Ni + 0.15% Sb

Both Ni + 0.15% Sb alloys failed in creep by formation of grain boundary cracks, however, in the AMDC heat there was evidence of ductile failure of intercavity ligaments during the final stage of creep failure. Figure 7 shows an optical micrograph of the internally cracked gage section from the LFZR specimen. The AMDC and LFZR heats had $\varepsilon_f$ of 26 and 32% respectively. Time to failure ($t_f$) was much greater in LFZR alloy (172 ks) than in the AMDC alloy (19 ks).

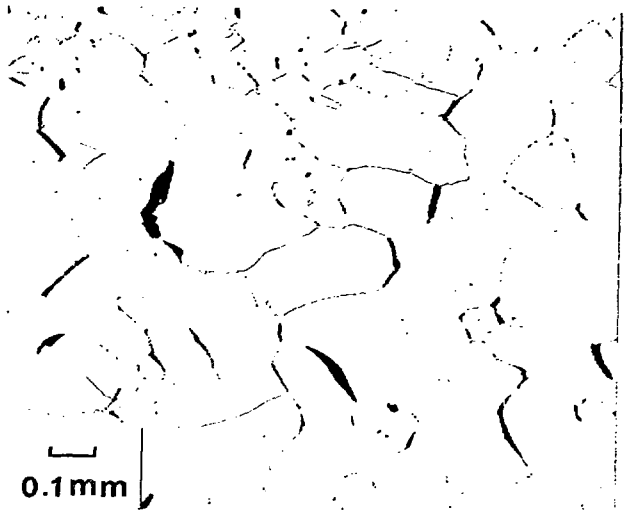


FIG. 7. Optical micrograph of LFZR-Ni + 0.15% Sb crept to failure at 595°C and 100 MPa.

Figure 8 shows two different areas on the AES fracture surface of the LFZR-Ni + 0.15% Sb. Both areas are contained within rounded depressions that we have labeled as cavities. The area in Fig. 8(a) is noticably rougher than the area in Fig. 8(b). Auger spectra from these two regions are shown in Fig. 9. Clearly the rough region exhibits a stronger S peak (~9 at. % S) than Sb peak (~3 at. % Sb), while the two peaks are more-or-less equal (7% S and 9% Sb) in smooth area [Fig. 8(b)].

Similar AES results were obtained from the AMDC-Ni + 0.15% Sb, however the AES fracture surface did not have as well defined rounded depressions corresponding to creep-induced cavities and cracks. Auger spectra similar to both spectra in Fig. 9 were obtained at various locations on the fracture surface, but contrasting rough and smooth areas were not found. Sputter etching less than ten atom layers from the fracture surface removed all of the S and Sb that was observed on both of the "as fractured" specimens.

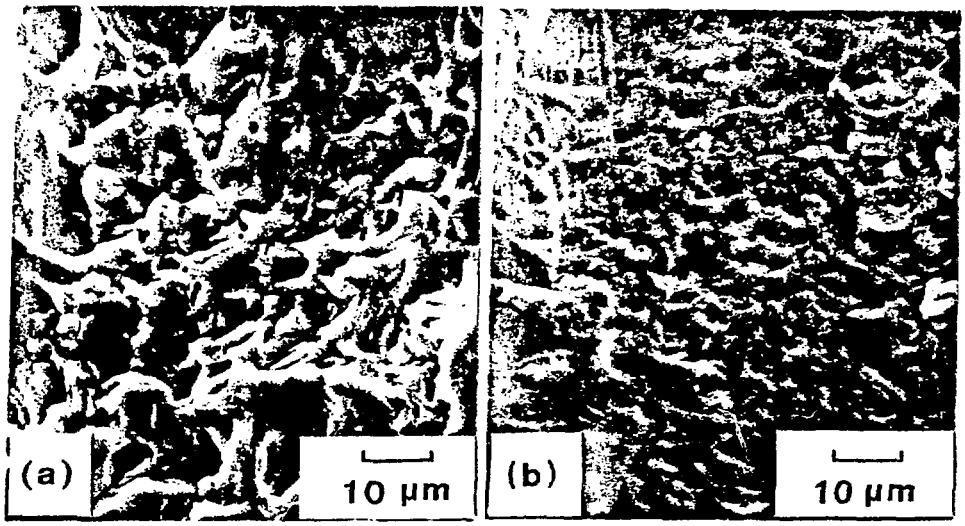


FIG. 8. The SEMs showing (a) rough and (b) smooth portions of the AES fracture from LFZR-Ni + 0.15% Sb.

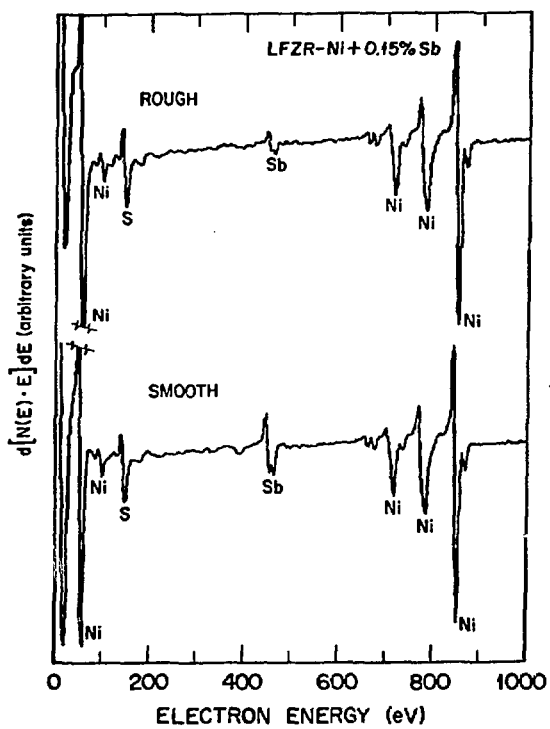


FIG. 9. Auger spectra from rough and smooth regions of LFZR-N + 0.15% shown in Fig. 8.

## 5. DISCUSSION

Creep test, and AES results, for each of the alloys, as well as results for a Ni + 1% Sb alloy studied previously [4-6], are summarized in Table 1.

Table 1. Summary of Creep and AES Results

| Alloy | Creep Test Results | | Composition (atom fraction) Bulk | | Cavity Surface | |
|---|---|---|---|---|---|---|
| | $\epsilon_f$(%) | $t_f$(ks) | Sb | S | Sb | S |
| Fe + 15% Ni + 15% Cr | 52 | 220 | $<23 \times 10^{-6}$(b) | $7 \times 10^{-6}$ | ND(a) | 0.23 |
| Fe + 15% Ni + 15% Cr + 1% Sb | 18 | 171 | $6 \times 10^{-3}$ | $35 \times 10^{-6}$ | 0.10 | ND(a) |
| LFZR - Ni + 0.15% Sb | 32 | 172 | $0.7 \times 10^{-3}$ | $9 \times 10^{-6}$ | 0.034 | 0.093 |
| AMDC - Ni + 0.15% Sb | 26 | 19 | $0.7 \times 10^{-3}$ | $9 \times 10^{-6}$ | 0.05 | 0.112 |
| Ni + 1% Sb | 9 | 27 | $4.2 \times 10^{-3}$ | $55 \times 10^{-6}$ | 0.026 | 0.225 |

(a) ND = not detected.
(b) Estimate from similarly prepared heats using same melt stock.

Perhaps the single most important observation concerning these results is that extensive segregation of either the intentionally added metalloid (Sb), a residual impurity (S), or both, was observed at cavity surfaces in all cavitated specimens.

An important question regarding the significance of these observations concerns when the observed segregation occurred. Studies of S and Sb segregation to external free surfaces in the Ni + 1% Sb alloy and the undoped Ni control heat indicate that Sb levels on a free surface reach ~80% of the steady state level in 5 to 10 minutes at 600°C, while S requires 20 to 25 minutes to approach steady state [9]. Based on this observation, we feel that the segregation observed here is representative of a cavity or crack surface composition for all but the first few minutes of its existence. Such segregation will directly influence cavity growth kinetics through its effects on surface diffusion and surface energetics. At this time, we can only speculate concerning the extent to which surface segregation reflects grain boundary segregation in these alloys. Any grain boundary segregation would, of course, influence cavity surface composition during its earliest stages.

### 5.1 Fe + 15% Ni + 15% Cr Alloys

The strong S segregation observed in the "undoped" alloy exemplifies the pronounced impurity segregation that commonly goes unnoticed in nominally pure alloys. In the absence of AES analyses such as those presented here, one

might have been tempted to site the behavior of the undoped alloy as evidence for "intrinsic" grain boundary cavitation and cracking. Given the intense S segregation indicated in Fig. 4, however, one must admit the possibility that the residual S plays a key role in the cavitation process.

The absence of detectable S on the cavities of the Sb doped alloy, in spite of its larger bulk concentration, indicates that Sb can inhibit S segregation to free surfaces in Fe + 15% Ni + 15% Cr. The detrimental effect of the Sb addition on creep ductility correlates directly with its segregation to cavity surfaces.

The slight enrichment of Ni on cavity surfaces to which Sb segregated (Sb doped alloy) is consistent with other observations of cosegregation of these elements in temper embrittled low alloy steels [10]. We are not aware of any reported interactions between S and Cr, such as observed for the undoped alloy; however, simple electronegativity considerations suggest that S has a stronger affinity for Cr than for Fe or Ni.

## 5.2 Ni + 0.15% Sb Alloys

Segregation in both Ni + 0.15% Sb alloys was about the same, and qualitatively similar to that observed previously in Ni + 1% Sb. Even though the Ni + 0.15% Sb has less Sb in solution than Ni + 1% Sb, segregation of Sb was somewhat more intense in the Ni + 0.15% Sb alloys. We attribute the increased Sb segregation in the Ni + 0.15% Sb to reduced competition by S for the available surface sites. The lower S levels in the Ni + 0.15% Sb should lead to less S segregation, leaving a larger fraction of surface sites available for occupation by Sb.

Although we have stated that AES fractures of intercavity ligaments exhibited no regions that were clearly intergranular, we would suggest that smooth areas such as the one in Fig. 8(b) might actually be areas where the ligament fractured partially along the boundary adjacent to the cavity before undergoing rupture via plastic instability. Our observations concerning the relative intensities of the S and Sb Auger signals are consistent with our previous results on Ni + 1% Sb if we make this assumption [5,6]. The roughness in Fig. 8(a) may, in fact, be related to the faceting that we previously observed on cavity surfaces of Ni + 1% Sb. For this reason, we have chosen the spectrum from the region of Fig. 8(a) as indicative of the cavity surface composition in Table 1.

Finally, the relationship between S segregation, Sb segregation, and creep cavitation appears to be more complex in the Ni-Sb alloys than in the Fe-Ni-Cr-Sb alloys. In both

systems, the effect of Sb additions is to reduce ductility and promote cavitation and cracking. In Ni + 0.15% Sb, however, the degree of ductility loss and cavitation correlates more directly with the extent of S (rather than Sb) segregation to cavity surfaces.

## 6. ACKNOWLEDGEMENTS

We wish to acknowledge the assistance of R. A. Padgett, B. F. Oliver, and R. L. Heestand in various phases of the experimental work, and C. L. Dowker and B. Stevens for manuscript preparation. Financial support of U.S. DOE-OBES-Division of Materials Sciences under contract W-7405-eng-26 with Union Carbide Corporation is also gratefully acknowledged.

## References

1. HOLT, R.T. and WALLACE, W., Int. Met. Rev., March 1976, 203, 1–24.

2. THOMAS, G.B. and GIBBONS, T.B., Metals Technology, March 1979, 95–101.

3. YOO, M.H., WHITE, C.L. and TRINKAUS, H., "Interfacial Segregation and Fracture," in Flow and Fracture at Elevated Temperatures, to be published by ASM, Metals Park, Ohio.

4. WHITE, C.L. and PADGETT, R.A., Scr. Metall., 1982, 16, 461.

5. WHITE, C.L. and PADGETT, R.A., Acta Metall., 1983, 31, 1005.

6. WHITE, C.L., SCHNEIBEL, J.H., and PADGETT, R.A. Metall. Trans. A., 1983, 14A, 595.

7. STEIN, D.F., JOHNSON, W.C. and WHITE, C.L., in "Grain Boundary Structure and Properties," (Ed. by G.A. Chadwick and D.A. Smith), Academic Press, London, 1976, pp. 301–351.

8. DAVIS, L.E., et al., "Handbook of Auger Electron Spectroscopy," Physical Electronic Industries, Eden Prairie, Minnesota, 1976.

9. WHITE, C.L. and LOSCH, W., unpublished research, Universidade Federal do Rio de Janeiro, Brazil.

10. GUTTMAN, M. and MCLEAN, D. in "Interfacial Segregation," (Ed. by W.C. Johnson and J.M. Blakely), ASM, Metals Park, Ohio, 1979, p. 261–348.